J Mater Sci (2010) 45:1823–1829
DOI 10.1007/s10853-009-4165-5

The role of tungsten in the coarsening behaviour of $M_{23}C_6$ carbide in 9Cr–W steels at 600 °C

Sadhan Ghosh

Received: 21 October 2009 / Accepted: 23 December 2009 / Published online: 12 January 2010

Abstract Tungsten is sometimes used as a solute in the so called 9Cr creep-resistant steels for use in the power generation industry, in part because of its ability to reduce the coarsening rate of $M_{23}C_6$ carbides. The mechanism by which it does so is not fully understood and indeed has been shown to be inconsistent with multicomponent coarsening theory, which predicts an opposite effect. This makes the role of tungsten to the coarsening behaviour of the carbide remain unsolved over decades. The work presented here is an attempt to show that the influence of tungsten can be reconciled with experiments, if kinetic study ignores the presence of Laves phase (Fe_2W) in the system.

Introduction

In some interesting work, Abe [1] characterised the evolution of the size of $M_{23}C_6$ particles in a series of experimental ferritic 9Cr steels as a function of tungsten concentration and time at 600 °C. He observed that for any combination of time and temperature, the size of the carbides decreased as the tungsten concentration is increased, and argued that this might be consistent with the classical coarsening theory designed for binary systems. Bhadeshia [2] later analysed the results and demonstrated that theory remains inconsistent with observations, which predicts an opposite effect, when the latter is formulated for multicomponent systems. Tungsten containing steels also precipitate Laves phase in addition to the carbide. Bhadeshia therefore speculated that a multiphase coarsening theory is needed to cover possible interactions between Laves phase and $M_{23}C_6$ particles. Laves phase is less coherent with the matrix, so there may exist a flux of solute from Laves phase to the carbide, resulting in a reduction in the coarsening rate of the carbide. The purpose of the present work is to investigate this proposal through a simulation of multicomponent coarsening in the context of experimental data [1] by Abe.

The simulation is conducted using *Dictra*, which is an established software for dealing with diffusion in multicomponent systems [3]. It has in the past been used to deal with many moving boundary problems, such as dissolution [4], growth [5, 6] and solidification [7], besides coarsening of carbides in two-phase systems, assuming local equilibrium at the interfaces [8, 9]. The estimation of equilibrium parameters accesses data from the phase diagram calculations using *Thermo-calc* [10]. Although there has been previous work on the coarsening of $M_{23}C_6$ [8, 11, 12] and Laves phase [6], the role of the latter to the coarsening behaviour of the carbide does not seem to have been addressed. This motivates for a kinetic study on the controversial role of Laves phase, as technological importance [1, 2, 5, 6, 8] of these 9Cr type steels are immense and theory [2] fails to elucidate this phenomena [1].

Experimental information

The steel compositions studied are listed in Table 1, and detailed in Ref. [1]. The initial size (R_0) of $M_{23}C_6$ particle was primarily taken to be 0.07 μm, following Abe [1]; later to compare simulation with the data [1], R_0 was estimated through extrapolation of the linear variation of the cube of particle radius versus time for alloys containing different level of tungsten.

S. Ghosh (✉)
Graduate Institute of Ferrous Technology, Pohang University of Science and Technology, Pohang 790-784, Republic of Korea
e-mail: sadhanghosh@postech.ac.kr

Table 1 Chemical compositions in wt%

Alloy	C	Cr	W
9Cr	0.104	8.96	–
9Cr–1W	0.101	9.01	0.99
9Cr–2W	0.100	8.92	1.92
9Cr–4W	0.101	9.09	3.93

The steel specimens were originally rod samples. They were austenitized, quenched, and then tempered to get 100% tempered martensite in all the alloys, except for 9Cr–4W steel, which contains 10 volume percent of δ-ferrite additionally in the microstructure.

Thermodynamic calculations

Equilibrium calculations were performed with *Thermo-calc* using *SGTE* database. As shown in Table 2, and as is well-known, the addition of tungsten increases the tendency to form Laves phase. However, the amount of $M_{23}C_6$ is not found to be sensitive to the tungsten content in the alloys.

Table 2 Calculated equilibrium compositions and phase quantities in wt% at 600 °C, using *Thermo-calc*

	Ferrite	$M_{23}C_6$	Laves
9Cr			
Fe	92.32	17.62	
C	0.00	5.61	
Cr	7.68	76.76	
wt% phase	98.15	1.85	–
9Cr–1W			
Fe	91.49	15.2	30.38
C	0.00	5.21	0.00
Cr	7.82	69.52	7.09
W	0.69	10.06	62.53
wt% phase	97.87	1.93	0.19
9Cr–2W			
Fe	91.56	15.27	30.41
C	0.00	5.21	0.00
Cr	7.75	69.42	7.05
W	0.69	10.10	62.53
wt% phase	96.38	1.92	1.70
9Cr–4W			
Fe	91.38	15.08	30.32
C	0.00	5.22	0.00
Cr	7.93	69.70	7.14
W	0.69	9.99	62.54
wt% phase	93.12	1.93	4.95

Coarsening model

Coarsening calculations were performed using *Dictra* software [13]. In a two-phase system, the method assumes a single particle at the centre of a spherical cell which is roughly 1.5 times larger than the average size (R_0) of the particle [14–16]. A contribution from interfacial energy is added to the Gibbs energy function for the particle:

$$\Delta G_m = \frac{2\sigma V_m}{r} \quad (1)$$

where σ is the interfacial energy in J m^{-2}, r the particle radius in m, and V_m the molar volume in m^3 mol^{-1}. In the present work, σ is assumed for $M_{23}C_6$ and Laves phase to be 0.7 and 1 J m^{-2}, respectively [11, 16]. The molar volume, V_m is given by:

$$V_m = \frac{V_{cell} \times N_A}{N} \quad (2)$$

where V_{cell} is the volume of a crystallographic unit cell, N_A the Avogadro's number and N the total number of atoms per unit cell. Volume fraction of the equilibrium phases was calculated assuming that substitutional elements only contribute volume to the system. This indicates that the volume fraction of $M_{23}C_6$ though remains constant that of Laves phase increases considerably with higher tungsten content in the alloys (Fig. 1).

The theory of diffusion-controlled precipitate coarsening was developed by Greenwood [14], Wagner [15] and Lifshitz and Slyozov [16]. The derivations are too lengthy to repeat, but the resulting rate equation is:

$$R^3 - R_o^3 = \frac{8DC_e\sigma V_m^2}{9RT}t = Kt \quad (3)$$

where R is the particle size after time t, D the diffusivity coefficient, C_e the equilibrium solute concentration, R the

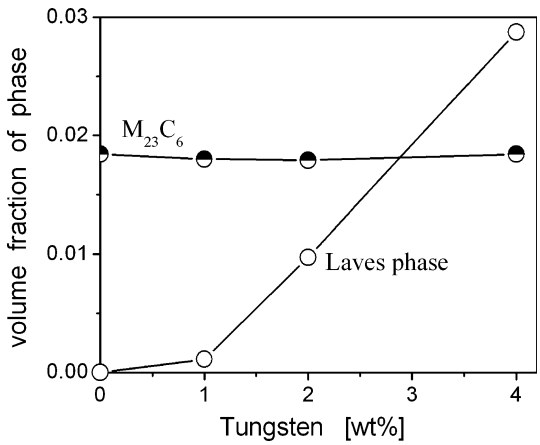

Fig. 1 Volume fraction of the equilibrium phases as a function of W-content in the alloys at 600 °C

universal gas constant, T the temperature and K the coarsening rate in $m^3\ s^{-1}$.

The present calculation assumes that coarsening occurs by volume diffusion alone. The key elements constituting the equilibrium phases were included to compare simulation with the experimental data. The tempered martensite matrix was approximated as ferrite; this is to justify the fact that tempering was performed over longer duration of time and previous authors [1, 11] also assumed the same.

Simulation ignoring Laves phase

The simulation is set up as a closed system with a spherical $M_{23}C_6$ particle, surrounded by ferrite, at the centre of the cell (Fig. 2). Although the particle size may change, the assumed spherical shape is maintained throughout the calculation. The initial conditions include the chemical compositions (Table 2) and size of the cell.

The present calculation has been devised in such a way that Laves phase be initially ignored in the simulation to exclude its role. As a result, if only $M_{23}C_6$ is in equilibrium with ferrite (Fig. 2), the following equations hold:

$$V_f^{M_{23}} = \frac{V_{M_{23}}}{V_2} = \frac{R_1^3}{R_2^3} \tag{4}$$

or,

$$R_2 = \frac{R_1}{\sqrt[3]{V_f^{M_{23}}}} \tag{5}$$

where $V_{M_{23}}$ and $V_f^{M_{23}}$ are the volume and volume fraction of $M_{23}C_6$, V_2 is the volume of cell and $R_1 = 1.5R_0 = 0.105$ μm. The cell size, R_2 is thus calculated and listed in Table 3 along with $V_f^{M_{23}}$ as a function of tungsten content in the alloys at 600 °C.

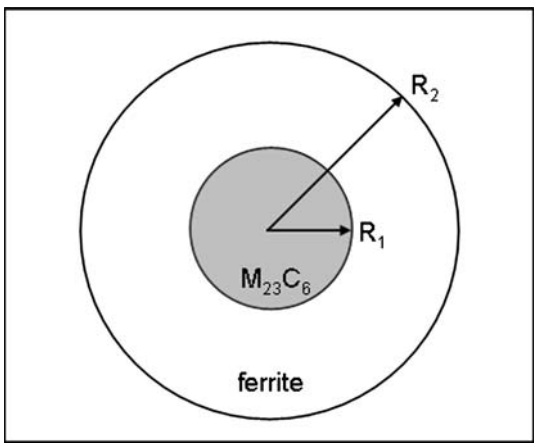

Fig. 2 A closed system, displaying a $M_{23}C_6$ particle of radius R_1 at the centre of a cell with radius, R_2

Table 3 Calculated cell size and volume fraction of $M_{23}C_6$ particle, ignoring Laves phase in the system at 600 °C

Alloy	$V_f^{M_{23}}$	R_2 (μm)
9Cr	0.0184	0.397
9Cr–1W	0.0180	0.400
9Cr–2W	0.0179	0.401
9Cr–4W	0.0181	0.400

Coarsening involves diffusion of atoms. When $M_{23}C_6$ is in equilibrium with ferrite there is no difference in chemical potential across the interface between matrix and the carbide. The alloy components can easily diffuse near the interface. The reaction rate will depend on how much solute flux being diverted from matrix to the carbide phase and vice versa. The concept of mass balance needs to be applied here. This job is systematically done by solving diffusion equation and the flux balance equations by *Dictra*. For more details, see Refs. [5, 6, 11].

Calculations were performed up to 10^7 s, which roughly equals 2,800 h consistent with the slow coarsening kinetics of $M_{23}C_6$ particle at 600 °C [12]. Diffusivity data were obtained from a multicomponent diffusion databank, *MOB2* associated with *Dictra*; this database had been used previously by many authors in calculating diffusion-controlled coarsening of $M_{23}C_6$ particle in creep-resistant steels [12, 17, 18].

Figure 3 demonstrates variation of the cube of particle radius, R^3 for alloys, containing 0–4 wt% of tungsten at

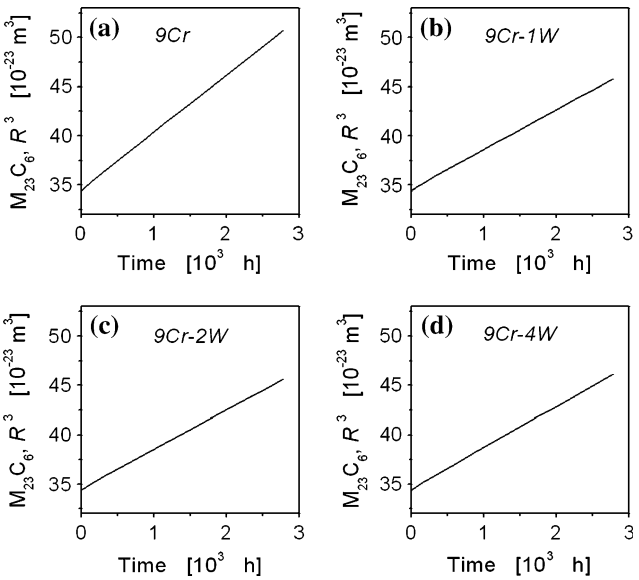

Fig. 3 Coarsening of $M_{23}C_6$, showing linear variation of the cube of particle radius, R^3 versus time in 9Cr–XW (X = 0–4 wt%) steels at 600 °C. The magnitude of coarsening in **b** 1% W is nearly same as that of **c** 2% W and **d** 4% W, but still lowers than **a** 0% W

600 °C. The linear correlation agrees with Eq. 3 to illustrate that there is a small reduction in the coarsening rate on the addition of the first level of tungsten, with little change beyond 1 wt% W. This is not entirely consistent with experimental observation [1], particularly for the alloys with higher level of tungsten. A possible reason could be

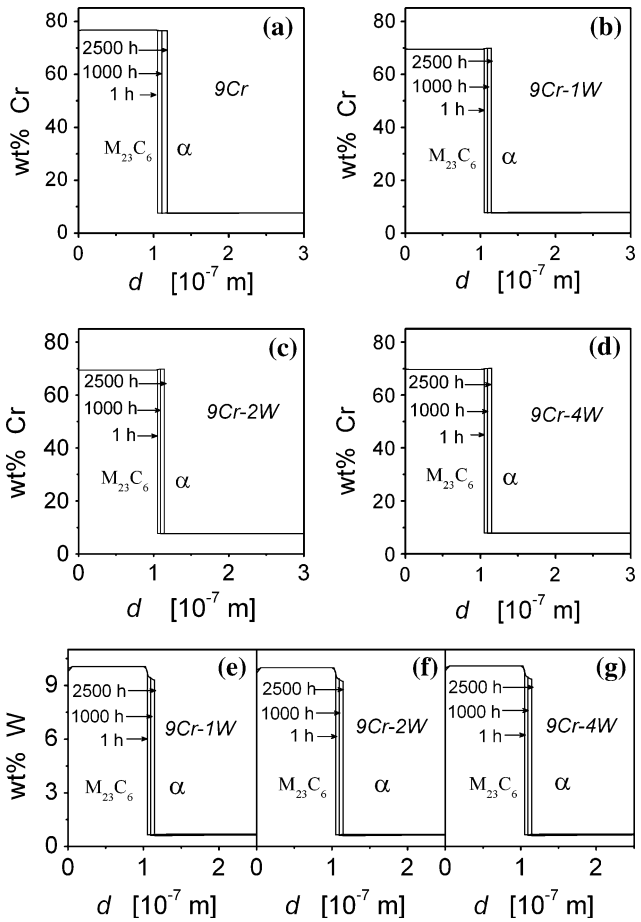

Fig. 4 *Concentration–distance* (*d*) profile, showing variation of **a**, **b**, **c**, **d** Cr and **e**, **f**, **g** W across the interface between $M_{23}C_6$ and ferrite matrix at 600 °C. The interface movement follows *arrow* directions as a function of time

that σ assumed for the carbide phase in all the alloys to be 0.7 J m^{-2}. This is a rigid assumption, as there is no literature data available on σ as a function of tungsten content in the alloys and it is indeed difficult to measure σ exactly either by experiment or numerical calculation, had been commented earlier by the previous author [1]. Therefore, the change of the particle size observed in Fig. 3 is mainly due to the composition effect, because V_m too assumed constant for all the alloys. This brings contribution (Fig. 4) of the key alloying elements into an inspection here.

Figure 4 illustrates variation of solute concentration across the interface between ferrite matrix and the carbide phase at different time intervals, starting from 1 to 2,500 h. It is clear from Fig. 4a that $M_{23}C_6$ maintains equilibrium Cr-concentration (~77%) through out the coarsening period, and so does ferrite (7.7%) in accordance with the *Thermo-calc* calculation (Table 2). It then decreases a bit with the addition of first level of tungsten, followed by nearly a constant trend up to 4 wt% of tungsten (Fig. 4b–d) is consistent with the reaction kinetics in Fig. 3b–d. A similar *concentration–distance* profile, when plotted for W, exhibits that tungsten level in $M_{23}C_6$ falls short of equilibrium concentration (~10%) ever since coarsening of the carbide begins (Fig. 4e–g). A possible reason could be slow diffusivity of W compared to Cr in these creep-resistance steels at 600 °C. The next step will be to include Laves phase in the simulation precipitated by tungsten in the solid solution.

Simulation including Laves phase

Generally, *Dictra* calculation concerns with two-phase simulation and it uses Eq. 5 to estimate the cell parameter [6, 11, 18]. Here to include Laves phase is the first of its kind, considering both $M_{23}C_6$ and Laves phase are in equilibrium with the ferrite matrix (Fig. 5). Note that the 9Cr alloy is excluded from the calculations because of the absence of Laves phase, also in the cell size calculation.

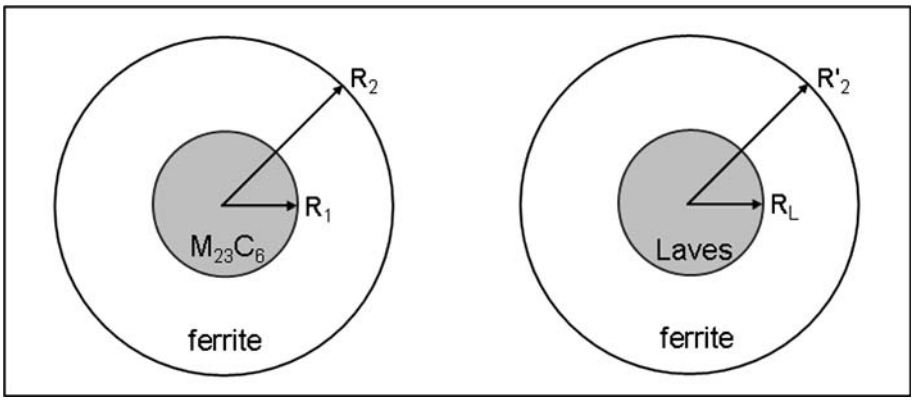

Fig. 5 A closed system with two spherical cells: one with a $M_{23}C_6$ carbide and other with a Laves phase particle at the centre of the cell, containing ferrite as the matrix phase

If V_L and V_f^L and are the volume and volume fraction of Laves phase, the following equation holds:

$$\frac{V_{M_{23}}}{V} + \frac{V_L}{V} = V_f^{M_{23}} + V_f^L$$

or,

$$V = \frac{V_{M_{23}} + V_L}{V_f^{M_{23}} + V_f^L} \tag{6}$$

where system volume, $V = (V_{M_{23}} + V_L + V_F)$ and volume of the matrix is V_F, to correlate with Eq. 6 as following:

$$V_{M_{23}} + V_L + V_F = \frac{V_{M_{23}} + V_L}{V_f^{M_{23}} + V_f^L}$$

or,

$$V_F = (V_{M_{23}} + V_L)\left[\frac{1}{V_f^{M_{23}} + V_f^L} - 1\right] = \frac{4\pi}{3}(R_1^3 + R_L^3)\left(\frac{V_f^F}{V_f^{M_{23}} + V_f^L}\right) \tag{7}$$

where V_f^F is the volume fraction of ferrite and R_L the size of Laves phase. Now, V_F will be shared between $M_{23}C_6$ and Laves phase by approximately ratio of their volume fractions to calculate the cell size. Therefore, if V' is the volume of ferrite to be occupied by $M_{23}C_6$, then

$$V' = \frac{4\pi}{3}\left(\frac{V_f^{M_{23}}}{V_f^{M_{23}} + V_f^L}\right)(R_1^3 + R_L^3)\left(\frac{V_f^F}{V_f^{M_{23}} + V_f^L}\right) \tag{8}$$

V' may also be obtained from Fig. 5 to correlate with Eq. 8 as following:

$$\frac{4\pi}{3}(R_2^3 - R_1^3) = \frac{4\pi}{3}\left[\frac{V_f^{M_{23}} V_f^F (R_1^3 + R_L^3)}{(V_f^{M_{23}} + V_f^L)^2}\right]$$

or,

$$R_2 = \sqrt[3]{\left(R_1^3 + \frac{V_f^{M_{23}} V_f^F (R_1^3 + R_L^3)}{(V_f^{M_{23}} + V_f^L)^2}\right)} \tag{9}$$

where R_2 is the cell size of $M_{23}C_6$, listed in Table 4. Similarly, cell size of Laves phase, R_2' (Table 4) may be calculated using the relation:

Table 4 Calculated cell size of $M_{23}C_6$ particle (R_2) and Laves phase (R_2') as a function of the alloy compositions at 600 °C

Alloy	$M_{23}C_6$		Laves phase	
	$V_f^{M_{23}}$	R_2 (μm)	V_f^L	R_2' (μm)
9Cr–1W	0.0180	0.484	0.0011	0.200
9Cr–2W	0.0179	0.378	0.0097	0.310
9Cr–4W	0.0181	0.270	0.0284	0.312

$$R_2' = \sqrt[3]{\left(R_L^3 + \frac{V_f^L V_f^F (R_1^3 + R_L^3)}{(V_f^{M_{23}} + V_f^L)^2}\right)} \tag{10}$$

where $R_L = 1.5R_0$. Since, R_0 of Laves phase is not available in Ref. [1] it is assumed to be the same as that of the carbide.

If $N_{M_{23}}$ and N_L are the total numbers of $M_{23}C_6$ and Laves phase particle in the system volume, V, the following equations hold:

$$\frac{N_{M_{23}} \times V_{M_{23}}}{V} = V_f^{M_{23}}$$

or,

$$N_{M_{23}} = \frac{V_f^{M_{23}} \times V}{V_{M_{23}}} \tag{11}$$

Similary,

$$N_L = \frac{V_f^L \times V}{V_{M_{23}}} \tag{12}$$

where V is obtained from the *Thermo-calc* calculations to state that $N_{M_{23}}/N_L$ ratio increases considerably with tungsten content in the alloys, following which size of $M_{23}C_6$ particle may be finer with increasing tungsten content in the alloys (Table 5). The yielding is going to be testified later with the outcome of simulations conducted with (Fig. 6) or without (Fig. 3) consideration of Laves phase in the system.

Table 5 $M_{23}C_6$ and Laves phase particle ratio in the system volume, V, at 600 °C

Alloy	V (10^{-6} m^3)	$N_{M_{23}}$ (10^{19})	N_L (10^{19})	$N_{M_{23}}/N_L$
9Cr–1W	6.48	8.12	4.96	1.6
9Cr–2W	6.43	8.00	4.36	1.8
9Cr–4W	6.29	7.88	1.24	6.4

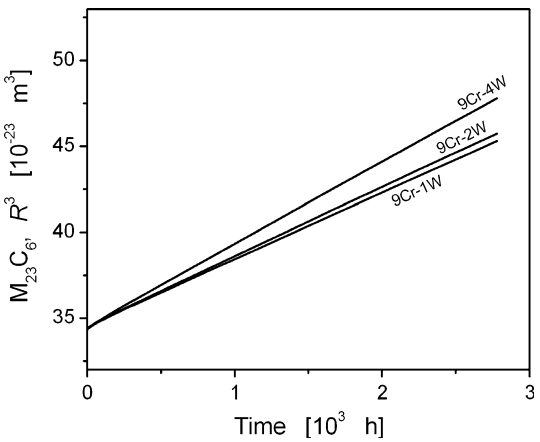

Fig. 6 Time-dependent coarsening of $M_{23}C_6$ particle at 600 °C, showing an opposite trend with experimental data [1] for the alloys containing 1–4 wt% of W, after taking Laves phase into accounts

Figure 6 illustrates coarsening of the carbide particle at 600 °C, after taking Laves phase into accounts for the alloys containing 1–4 wt% of tungsten. A linear correlation between R^3 and t can be seen consistent with Eq. 3. The result though exhibits a reverse trend that coarsening rate of $M_{23}C_6$ may accelerate with increasing tungsten content in the alloys. This disregards the experimental observation by Abe [1]. The reason is not fully clear because all the input parameters remain the same as that in Fig. 3 except change in cell size. Comparison of Tables 3 with 4 shows that R_2 decreases with rising tungsten content in the alloys while including Laves phase in the system; this may probably affect the diffusion distance. As an example, for the alloy containing 4 wt% W has the smallest matrix region (Table 4), so substitutional elements like Cr and W may traverse smaller distance to enhance coarsening rate of the carbide in Fig. 6.

An effort was also made to calculate simultaneous coarsening of $M_{23}C_6$ and Laves phase particles, assuming [5] both the cells in the same chemical potential. The simulation resulted numerical error similar to coarsening of Laves phase in ferrite; suggesting that latter for Laves phase may not be observed in this system. A similar fact was reported by Paul et al. [19], following an experimental investigation in Mo alloyed 9Cr steels that fine precipitates of Laves phase form at 500 °C after prolong duration of ageing. It takes nearly 10,000 h for precipitates to be clearly visible in TEM (Transmission Electron Microscopy). As a result, coarsening of $M_{23}C_6$ may occur independently at the early stage of coarsening, and if it has to affect coarsening, may be possible at a far longer duration due to encapsulation of $M_{23}C_6$ with Laves phase particle.

Accordingly, Krocakova et al. [20] performed energy-filtered transmission electron microscopy in 9Cr–W steel during ageing and creep test at 600 °C. There, only nucleation and growth of Laves phase were reported but its role to the coarsening behaviour of $M_{23}C_6$ could not be established. It is expected that precipitation of Laves phase (Fe_2W) mainly causes depletion of tungsten from solid solution; hence, contribution of the latter element to the solid solution strengthening may be lost until Laves phase induced by it further contributes to the precipitation strengthening [20].

Discussion

The present work details coarsening behaviour of $M_{23}C_6$ particle with (Fig. 6) or without (Fig. 3) considerations of Laves phase in multicomponent systems. Both experimental observation [1] followed by *Thermo-calc* calculation (Table 2) suggest that tungsten induces Laves phase in the system. However, to include latter in the simulation, an opposite trend (undesirable) with the experimental data was observed (Fig. 6). Interestingly, Bhadeshia [2] also predicted the same but for multicomponent systems, due to which inclusion of Laves phase was suggested in the calculation.

The role of Laves phase seems to be inconspicuous here because presence (Fig. 6) of the latter cannot elucidate this phenomenon [1]. Secondly, evidence is rare for coarsening of this intermetallic phase near 600 °C, so volume diffusion of solutes from Laves to the carbide phase cannot be established. A compelling argument to support this notion is that volume fraction of $M_{23}C_6$ is independent of Laves phase in the system (Fig. 1). Therefore, excluding Laves phase in the calculation seems to be more convincing to compare (Fig. 7) simulation with the experimental data.

Figure 7 finally compares simulation with the experimental data [1] for $M_{23}C_6$ particle size at 600 °C. Unlike other compositions, a better agreement was obtained for 9Cr–4W steel. This appeared to be confusing initially, because Fig. 7 basically repeats the same calculation as that in Fig. 3, where relative variation of R in 4 wt% W is comparable with 1–2 wt% of W and the maximum change should be obtained in 9Cr steel. A reason for the discrepancy is particle size (R_0) effect. The R_0 values estimated for different alloys indeed vary with the alloy compositions; it is minimum (0.07 μm) in 9Cr–4W steel to be maximum (0.35 μm) in the 9Cr steel. According to Eq. 1, particle of the largest size will have the lowest free energy state, and hence higher stability against coarsening to exhibit slow reaction rate of the carbide in Fig. 7. This fact is attributed to a numerical complexity which has to be faced by any computational technique, until R_0 for various alloys it taken to be equal or small, similar to that in Figs. 3 and 6.

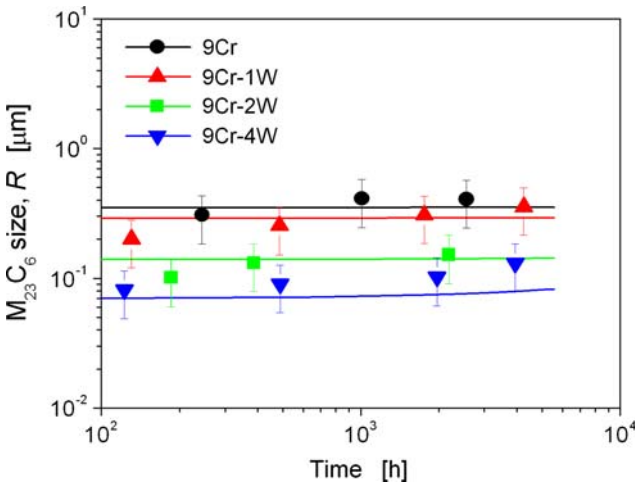

Fig. 7 Comparison of simulation (*line*) with experimental data (*symbol*) for $M_{23}C_6$ particle, showing better agreement in 9Cr–4W steel compared to others due to particle size (R_0) effect

This section will now investigate key parameters involved in the coarsening process to evaluate the rate controlling parameters. To do so, Eq. 3 may be approximated as following after excluding the constant terms, such that

$$R^3 - R_0^3 \approx DC_e\sigma V_m^2 t \quad (13)$$

where V_m is an input (0.62×10^{-5} m^3 mol^{-1}) besides σ. The variation of V_m is less likely to be a key parameter, because it does not alter much with the alloy compositions and V_m^2 is too small a quantity. Therefore, Eq. 13 may be further simplified as

$$R^3 - R_0^3 \approx k'(DC_e)t \quad (14)$$

where K' is proportionality constant to emphasise that the reaction kinetics, K, mainly depends on diffusivity (D) and equilibrium concentration (C_e) of the solutes, apart from σ. In the present calculation, C_e is obtained from *Thermo-calc* calculation using *SGTE* database and D is sourced from mobility database, *MOB2*, associated with *Dictra*. Therefore, if any discrepancy has to arise in the calculation it will be caused by either deficiencies in the databases or a simplification on the particle shape geometry, had been reported earlier by the previous authors [5, 6, 8].

Finally, it is imperative to note that the experimental work [1] originally proposed grain boundary diffusivity than bulk diffusivity used in the simulation. It is rather a compulsion because grain boundary diffusivity is not currently available in the mobility database, following which *Dictra* simulation performed by the previous authors [5–9, 11, 12, 18] used bulk diffusivity alone. However, to defend it, there still remains an argument that for any crystalline solid, the volume fraction of grain boundary area is generally much lower than the grain body. Therefore, majority of the solutes may diffuse from bulk to maintain equilibrium during the coarsening process. This provides slow diffusivity of the substitutional elements like Cr or W to emerge as a rate controlling parameter in these creep-resistant steels at 600 °C. Amongst them the role of tungsten will be the dominating one. A simple reason could be—when W-concentration in the alloys increases the volume fraction of Laves phase also increases (Fig. 1); i.e., precipitations of large numbers of Laves phase particles in the matrix. So, there will be a quick demand of tungsten for the latter process. In order to keep the supply intact, tungsten will preferentially go to Laves phase (Fe_2W) than to $M_{23}C_6$, which also needs tungsten (Table 2). This may enhance precipitation kinetics of Laves phase but coarsening rate of the carbide will be suppressed. Figure 4e–g clearly indicates that there is a shortage of tungsten in $M_{23}C_6$ to retard coarsening rate of the carbide in these creep-resistant steels at 600 °C.

Conclusion

The present work demonstrated that *Dictra* simulation can in principle explain the influence of tungsten on the coarsening behaviour of chromium-rich $M_{23}C_6$ particles in creep-resistant 9Cr type steels at 600 °C. This is an effort to consolidate experimental data presented by Abe and finally to resolve controversy on the role of Laves phase to the coarsening behaviour of the carbide. The simulation performed with and without Laves phase indicates that reaction kinetics agrees well with the experimental data when simulation ignores presence of Laves phase in the system. It will otherwise exhibit a trend completely opposite to the experimental data.

Acknowledgements The author is greatly indebted to Dr. H. K. D. H. Bhadeshia and Dr. H. S. Kim for discussion, suggestion and comments on the contents of this paper.

References

1. Abe F (1999) In: Sakai T, Suzuki HG (eds) Proceedings of the 4th international conference on recrystallization and related phenomena. JIM, Sendai, p 289
2. Bhadeshia HKDH (2001) ISIJ Int 41:626
3. Borgenstam A, Engstrom A, Hoglund L, Agren J (2000) J Phase Equlib 21:269
4. Liu Z-K, Höglund L, Jönsson B, Ågren J (1991) Met Trans A 22A:1745
5. Bjärbo A, Hättestrand M (2001) Metall Mater Trans A 32A:19
6. Bjärbo A (2003) Scan J Metall 32:94
7. Walter C, Hallstedt B, Warnken N (2005) Mater Sci Eng A 397:385
8. Gustafson Å, Hättestrand M (2002) Mater Sci Eng A 333:279
9. Gustafson Å (2000) Mater Sci Eng A 287:52
10. Sundman B, Jansson B, Andersson JO (1985) Calphad 9:153
11. Hu X, Li L, Wu X, Zhang M (2006) Int J Fatigue 28:175
12. Hald J, Korcakova L (2003) ISIJ Int 43:420
13. Raabe D (1998) Computation materials science. Wiley-Vch Verlag GmbH, p 231
14. Greenwood GW (1956) Acta Metall 4:243
15. Wagner C (1961) Z Elektrochemie 65:581
16. Liftshitz IM, Slyozov VV (1961) Chem Solids 35:35
17. Schneider A, Inden G (2005) Acta Mater 53:519
18. Gustafson Å, Ågren J (2001) ISIJ Int 41:356
19. Paul VT, Saroja S, Vijayalakshmi M (2008) J Nucl Mater 378:273
20. Korcakova L, Hald J, Somers MAJ (2001) Mater Char 47:111